Bioprocess and Biosystems Engineering (2023) 46:359–371
https://doi.org/10.1007/s00449-022-02743-7

RESEARCH PAPER

Intermolecular degradation of aromatic compound and its derivatives via combined sequential and hybridized process

Yen-Yie Lau[1] · Yee-Shian Wong[1,2] · Soon-An Ong[1,2] · Nabilah Aminah Lutpi[1,2] · Sung-Ting Sam[3] · Tjoon-Tow Teng[4] · Kim-Mun Eng[5]

Received: 12 January 2022 / Accepted: 6 June 2022 / Published online: 7 July 2022

Abstract

The under-treated wastewater, especially remaining carcinogenic aromatic compounds in wastewater discharge has been expansively reported, wherein the efficiency of conventional wastewater treatment is identified as the primary contributor source. Herein, the advancement of wastewater treatments has drawn much attention in recent years. In the current study, combined sequential and hybridized treatment of thermolysis and coagulation–flocculation provides a novel advancement for environmental emerging pollutant (EP) prescription. This research is mainly demonstrating the mitigation efficiency and degradation pathway of pararosaniline (PRA) hybridized and combined sequential wastewater treatment. Notably, PRA degradation dominantly via a linkage of reaction: thermal cleavage, deamination, silication and diazene reduction. Thermolysis acts as an initiator for the PRA decomposition through thermally induced bond dissociation energy (BDE) for molecular fragmentation whilst coagulation–flocculation facilitates the formation of organo-bridged silsesquioxane as the final degradation product. Different from conventional treatment, the hybridized treatment showed excellent synergistic degradability by removing 99% PRA and its EPs, followed by combined sequential treatment method with 86% reduction. Comprehensive degradation pathway breakdown of carcinogenic and hardly degradable aromatic compounds provides a new insight for wastewater treatment whereby aniline and benzene are entirely undetectable in effluent. The degradation intermediates, reaction derivatives and end products were affirmed by gas chromatography–mass spectrometry, Fourier transform infrared spectroscopy and ultraviolet–visible spectrophotometry (GC–MS, FTIR and UV–Vis). This finding provides valuable guidance in establishing efficient integrated multiple-step wastewater treatments.

Graphical abstract

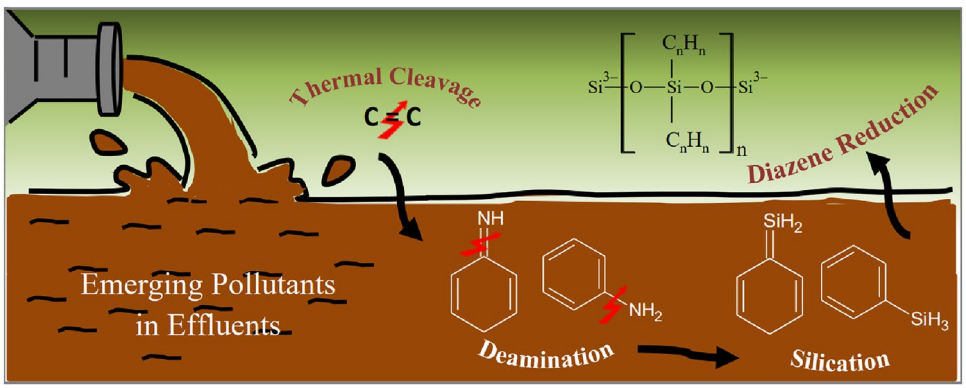

Keywords Emerging pollutants · Degradation · Wastewater treatment · Hybridized treatment · Combined sequential treatment

Extended author information available on the last page of the article

Abbreviations

B-MAC	Boron-doped mesoporous activated carbon
CF	Coagulation–flocculation
DBD	Dielectric barrier discharge
EPs	Emerging pollutants
FTIR	Fourier transform infrared spectroscopy
GC–MS	Gas chromatography–mass spectrometry
M.W.	Molecular weight
PRA	Pararosaniline
PZC	Point of zero charge
UV–Vis	Ultraviolet–visible spectrophotometry

Introduction

Dyes and their cleaved intermediates are considered as emerging pollutants (EPs) that are produced during textile activities [1]. Organic dyes are commonly used for all dyestuff concerning production and the metabolic activation of intermediates potentially generates carcinogenic and mutagenic substances [2, 3]. Aromatic compounds such as aniline and its derivatives are one of the anthropogenic persistent organic EPs that are harmful to the human central nervous system, liver and kidneys [4, 5]. Aromatic amines with an active metabolic amino group are classified as mutagenic since the hydroxylamine intermediate can cause DNA and protein damage [6]. Brüschweiler reported that there are approximately 588 mg/kg of aniline and 134 mg/kg 4-ethoxyaniline was measured in textiles [7].

Pertaining to the negative impacts, this had brought forth more progressively rigorous quality requirements for wastewater effluent. Therefore, industries hold the responsibility to ensure no under-treated wastewater was discharged [8]. However, production of the wastewater complexity derived with industrial development had caused limitation to several physical and chemical treatment methods which have been evaluated by researchers to treat aniline-rich wastewater. However, there were remaining untreated aniline derivatives present in the effluent, such as adsorption by activated kaolinite with 8% remaining [9], electro-catalytic oxidation using boron-doped mesoporous activated carbon (B-MAC) with 50–62% removal [10], photocatalytic using solar and UV-C artificial radiation equipped rotating drum reactor with 15% remaining [11], dielectric barrier discharge (DBD) plasma with 9.8% remaining [12]. Biological treatment has the capability to degrade 100% aniline by *Pigmentiphaga daeguensis* AN-4a, at a very low concentration of aniline (10 mg/L) for 15 h; however, the efficiency is too low to apply for industries [13].

The constraint that was encountered has made the single treatment method inadequate for the removal of aniline from industrial wastewater. Thus, it is necessary to improve wastewater treatment methodology to enhance wastewater reclamation. Researchers are constantly studying various combined or hybridized treatment methods to improve industrial wastewater treatment efficiency. The combined process is where two or more treatment methods are operating in sequential sequences of one after another. On the other hand, in a hybridized process one or more treatment methods are integrated into a one-time operation treatment. Reviews from few researchers revealed that combined or hybridized processes such as electro-oxidation and UV/H_2O_2, ultrasound and ozonation, electro-Fenton are more promising to treat aniline-rich wastewater [14–16].

Herein, PRA dye which had laboratory proved contained mutagenic compounds is used as amino model to evaluate the advanced treatment performance [17]. The advanced treatment applied in this study is combined and hybridized coagulation–flocculation (CF) and thermolysis processes. CF was selected since CF is the extensively used treatment method in industrial application, whereas thermolysis is used due to its specialty mechanism of thermal molecular structure decomposition. This research is primarily focused on the best-driven treatment methods of PRA-containing wastewater by elucidating the degradation kinetics. Besides, mineralization of the treatment methods is demonstrated and compared to identify the structural attributions towards PRA reduction.

Materials and methods

Chemicals and materials

Pararosaniline hydrochloride (PRA) of 323.83 $gmol^{-1}$ was supplied by Sigma-Aldrich (Selangor, Malaysia). 1000 mg/L concentration of PRA was prepared by dissolving 1 g of powder in 1000 mL of deionized water. Hydrochloric acid (HCl), sodium hydroxide (NaOH) and other analytical grade reagents were purchased from Fisher Scientific (M) Sdn. Bhd. (Selangor, Malaysia), and used without further purification.

Experimental procedure

Thermolysis

Thermolysis experiments were carried out using thermal catalytic reactor, see Fig. 1a. A 500 mL three-necked round bottom flask was heated using a stirring heating mantle (Mtops Model MS-ES303). A vertical water-cooled condenser was attached at the center of the three-necked round bottom flask to prevent loss of water through vaporization; one of the glass necks was attached with a temperature probe to observe the temperature stability and the other glass neck was enclosed and open for sample withdrawal when needed

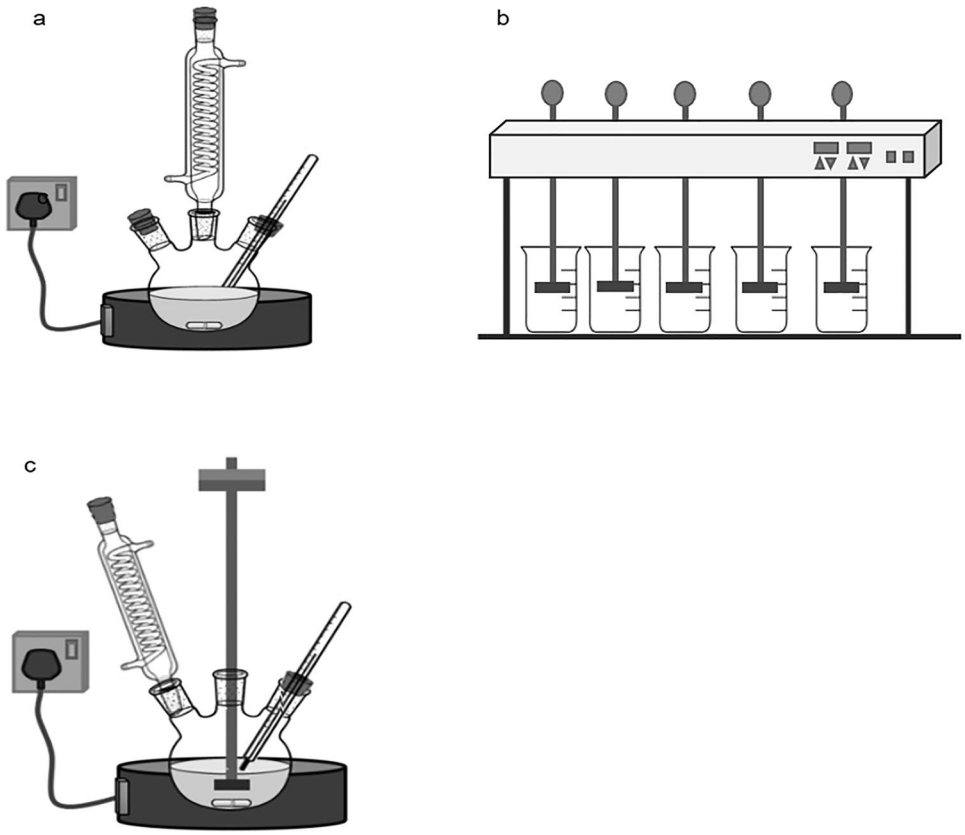

Fig. 1 Schematic diagram of **a** thermolysis, **b** coagulation–flocculation and **c** hybridized reactor

to collect the wastewater for analysis. While the sample was heated to desired temperature, a constant stirring speed using a magnetic stirrer in the rotamantle was constantly applied throughout the process to ensure the heating was in equilibrium state [18].

Coagulation–flocculation

Experiments on PRA wastewater were performed using Jar-Test equipment (JLT6 VELP Scientifica) for coagulation–flocculation, refer Fig. 1b. The previous study on optimum pH of silifloc (a.k.a laterite soil, bi-functionality natural coagulant–flocculant) was identified at pH 2, which was the point of zero charge (PZC) for silifloc to be activated [19]. The behavior of silifloc in treating PRA was investigated by varying the silifloc dosage. The mixtures were stirred rapidly at 200 rpm for 2 min, and then decreased to 100 rpm for 15 min. Subsequently, the mixtures were allowed to settle for 30 min.

Hybridized process

The thermolysis and coagulation–flocculation were carried out simultaneously using thermal catalytic reactor and an attached mixing stirrer. The lab-scale reactor was set up as shown in Fig. 1c. A 500 mL three-necked round bottom flask was heated using a stirring heating mantle (Mtops Model MS-ES303) and a mixing stirrer (IKA overhead Model RW20) was attached at the center of the three-necked round bottom, one of the glass necks was attached with water-cooled condenser and the other glass necks were attached with a temperature probe.

Experimental design

Experiments were carried out by designing the combined sequential and hybridized treatment methods stated as below:

(i) Thermolysis followed by coagulation–flocculation (thermolysis–CF) as a combined sequential treatment. The dye wastewater was first treated by thermolysis; hence, the thermolysis-treated wastewater was cooled to room temperature before proceeding to coagulation and flocculation. The treatment processes is illustrated in Fig. 1a followed by Fig. 1b.
(ii) Coagulation–flocculation followed by thermolysis (CF–thermolysis) as a combined sequential treatment. At first, the dye wastewater was treated with coagulation–flocculation, and then the mixture was filtered to collect the supernatant. Subsequently, the supernatant was treated with thermolysis process.

The process of treatments is presented in Fig. 1b followed by Fig. 1a.

(iii) Hybridized treatment process whereby the treatment processes of thermolysis and coagulation–flocculation are integrated into a single reactor to perform a simultaneous reaction on the dye wastewater as in Fig. 1c.

Analytics

pH values

The pH values of each sample were measured with a pH meter (826 pH mobile, Metrohm). The desired pH values were adjusted using HCl and NaOH.

PRA concentration

The concentration of PRA was analyzed by UV–Visible scanning spectrophotometry (Hitachi U-2810) and the UV–Vis absorption spectra were recorded from 200 to 800 nm. The PRA reduction efficiency was calculated using the correlation of baseline and final absorbance (Eq. 1) at the absorbance bands of 290, 232 and 545 nm.

$$\left[\frac{(A_o - A_t)}{A_o}\right] \times 100, \quad (1)$$

where A_o is the initial absorbance (abs) and A_t is the final absorbance (abs).

Degradation intermediates and products

The molecular formula and weight of the degradation intermediates and products were distinguished by gas chromatography–mass spectrometry, GC–MS (GC 2010 Plus, Shimadzu) equipped with BPX 5 capillary column (30 m length, 0.25 mm thickness and 0.2 mm internal diameter). Supernatant was extracted using dichloromethane, subsequent helium was used as the carrier gas at 220 °C injection temperature, meanwhile the column temperature was increased from 40 to 250 °C with 20 min holding time. The functional groups of the degradation products were analyzed using Fourier-transform infrared (Bruker Tensor II). FTIR was performed with total attenuated reflectance (ATR) from 4500 to 650 cm^{-1}. UV–visible scanning spectrophotometry (Hitachi U-2810) was used to study the degradation kinetics at the specific wavelength.

Statistical analysis

All experiments were carried out three times. One-way ANOVA was used to determine the significant level of the evaluated factors statistically. A threshold significance level, p value of 0.05, was applied to all the engineering parameter analysis.

Results and discussion

In the course of study, combined sequential treatment processes were performed in two successive steps with two means: thermolysis was followed by coagulation–flocculation (thermolysis–CF) and coagulation–flocculation was followed by thermolysis (CF–thermolysis). Taking the color reduction as the performance indicator, the effects of different pH values on the various treatments, reaction time and dosage of silifloc were investigated. The significance of the operating parameters correlation were statistically analyzed by ANOVA as shown in Table 1.

Thermolysis–CF treatment processes performance study

Figure 2 demonstrates the performance of thermolysis–CF under various experimental conditions. The effect of reacting thermolysis temperature on color reduction rate was carried out from pH 2 to 9 at thermolysis treatment time 30 min as shown in Fig. 2a and the factors are statistically significant because the p values are less than 0.05 as presented in Table 1. The color reduction rate increases with the increase of the initial pH of the PRA dye wastewater. When the pH reaches 9, color reductions are observed at the highest PRA removal rate for both temperatures, 23% at 60 °C and 39% at 90 °C. The temperature at 90 °C gives higher removal due to the presence of higher bond dissociation energy (BDE) to further break the stronger molecular bond and destabilize the PRA dye molecular structure [20]. The final pH after the treatment was also measured and a decrease in pH from its initial pH of 9 to pH 5.84 was observed. The reason for this phenomenon may attribute to the release of H^+ ion in solution during the course of catalytic hydrolysis [21] with cleavage of the PRA dye structure as the main conversion as shown in Eq. 2.

Table 1 ANOVA analysis of color reduction for (a) thermolysis–CF, (b) CF–thermolysis and (c) hybridized treatments

(a)	DF[a]	Adjusted SS[b]	Adjusted MS[c]	*F* value	*p* value*
pH	4	769.00	192.25	8.68	0.030
Temperature	1	176.40	176.40	7.96	0.048
Error	4	88.60	22.15		
Total	9	1034.00			
S	R^2	Adjusted R^2	Predicted R^2		
4.70638	91.43%	80.72%	46.45%		
(b)	DF[a]	Adjusted SS[b]	Adjusted MS[c]	*F* value	*p* value*
pH	4	7.000	1.750	11.670	0.018
Temperature	1	0.900	0.900	6.000	0.070
Error	4	0.600	0.150		
Total	9	8.500			
S	R^2	Adjusted R^2	Predicted R^2		
0.5	92.94%	84.12%	55.88%		
(c)	DF[a]	Adjusted SS[b]	Adjusted MS[c]	*F* value	*p* value*
pH	4	413.600	103.400	25.220	0.004
Temperature	1	67.600	67.600	16.490	0.015
Error	4	16.400	4.100		
Total	9	497.60			
S	R^2	Adjusted R^2	Predicted R^2		
2.02485	96.70%	92.58%	79.40%		

*Significant ($p < 0.05$)

[a]*DF* degree of freedom

[b]*SS* sum of squares

[c]*MS* mean square

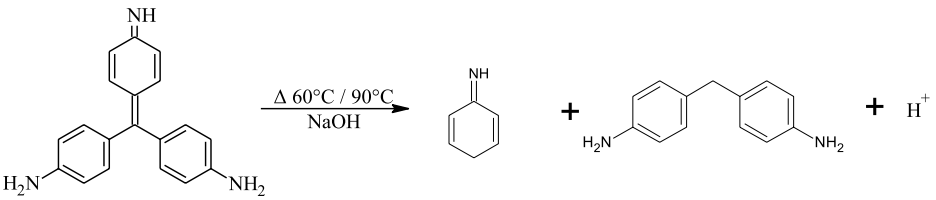

Pararosaniline — cyclohexa-2,5-dien-1-imine — 4,4'-methylenedianiline — Hydrogen ion

(2)

Unstable 4,4'-methylenedianiline tends to decompose to a more stable structure, aniline as shown in Eq. 3

With the presence of excessive H^+ during thermolysis, the release rate of NH_4^+ attached to the benzene rings also

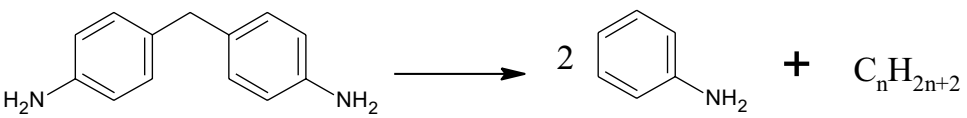

4,4'-methylenedianiline — Aniline — Methane

(3)

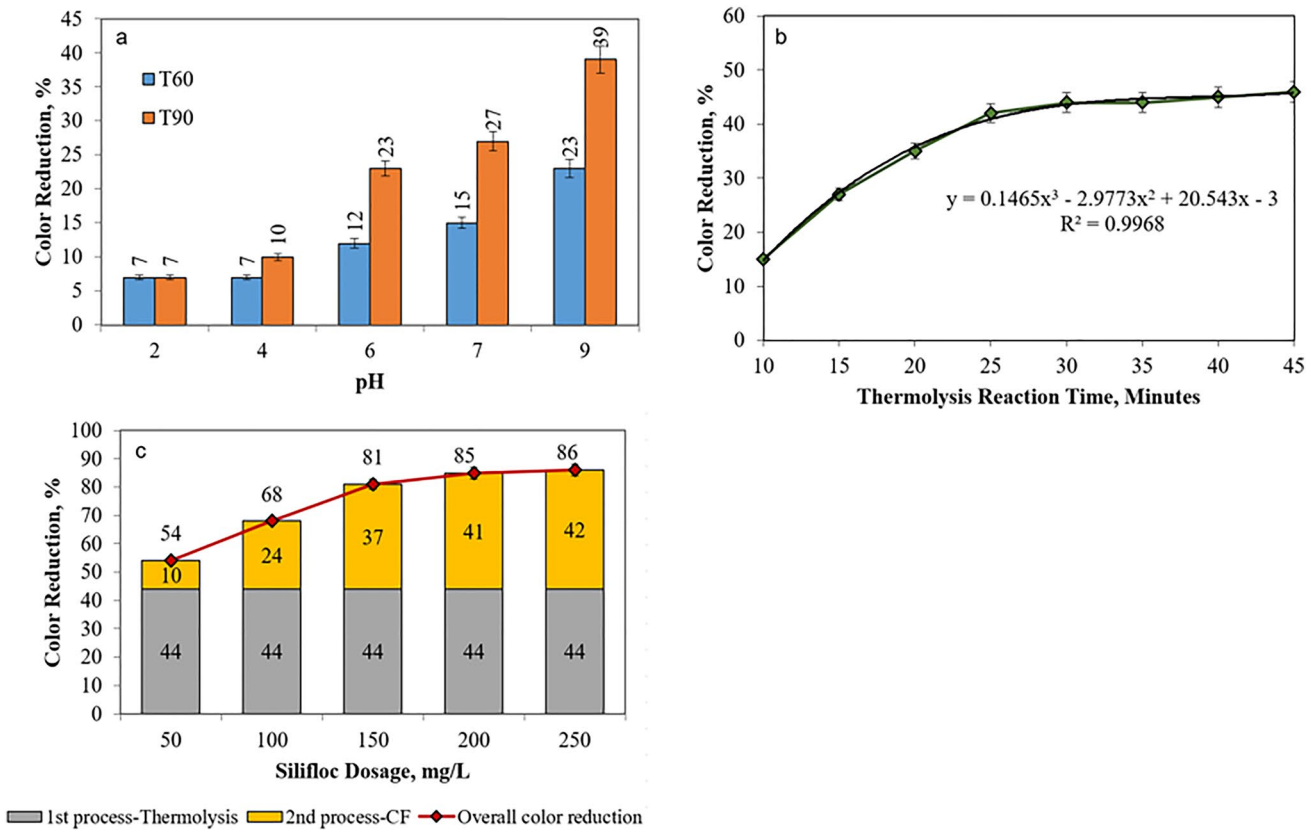

Fig. 2 Study of combined sequential treatment (thermolysis–CF). Effect of **a** PRA solution initial pH, **b** thermolysis reaction time and **c** silifloc dosage on color reduction rates

increases [22]. Attribution to the spontaneous hydrolytic deamination reaction is illustrated in Eqs. 4 and 5.

cyclohexa-2,5-dien-1-imine — 2,5-cyclohexadienone — Ammonium ion (4)

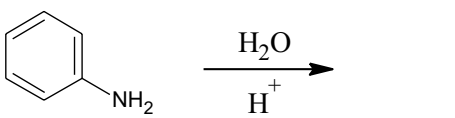

Aniline — Benzene — Ammonium ion (5)

The time course of the thermolysis treatment has been studied at the optimum pH as shown in Fig. 2b. The color

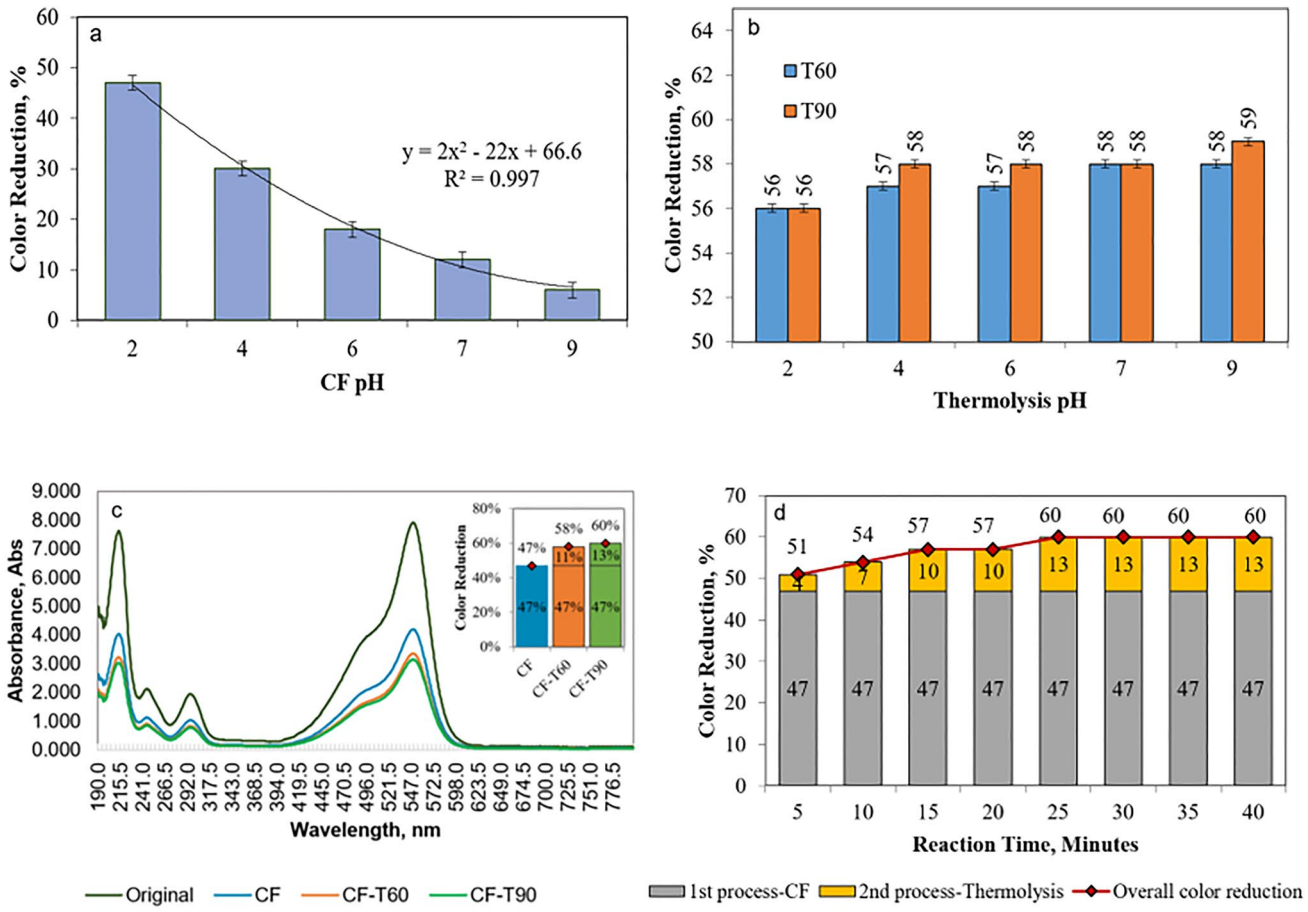

Fig. 3 Study of combined sequential treatment (CF–thermolysis). **a** Effect of PRA solution initial pH during CF. **b** Effect of thermolysis pH during thermolysis. **c** PRA degradation with different treatment processes. **d** Effect of reaction time on color reduction rates

reduction rate increases gradually with the increase of time until 30 min with a maximum PRA color reduction of 44%; no changes were observed beyond 30 min. This scenario may be because the organic molecules' decomposition has formed precipitation, and higher BDE is required to break through the surface area with stronger molecular bonding [23]. After thermolysis treatment, the pretreated (thermolysis) wastewater was subjected to the CF to study the combined effect. The PRA reduction efficiency through the CF process with respect to the dosage of coagulant silifloc is depicted in Fig. 2c. The color reduction rate increases as the silifloc dosages increase with a maximum pretreated wastewater removal of 42%. Therefore, the maximum color reduction for combined sequential thermolysis–CF is 86%.

CF–thermolysis treatment process performance study

CF–thermolysis performance under various operating parameters is depicted in Fig. 3. The initial pH wastewater is essential for CF owing to the effect on floc characteristics and coagulant hydrolysis mechanism. As can be seen in Fig. 3a, the effect of pH was carried out from pH 2 to 9 and the optimum pH is observed at pH 2 with a maximum color reduction rate of 47%; this fact was also verified by Lau et al. [19]. This can be ascribed to the reaction of cationic PRA, which tends to react with silica that presents in the form of SiO_3^{2-} in Eq. 6:

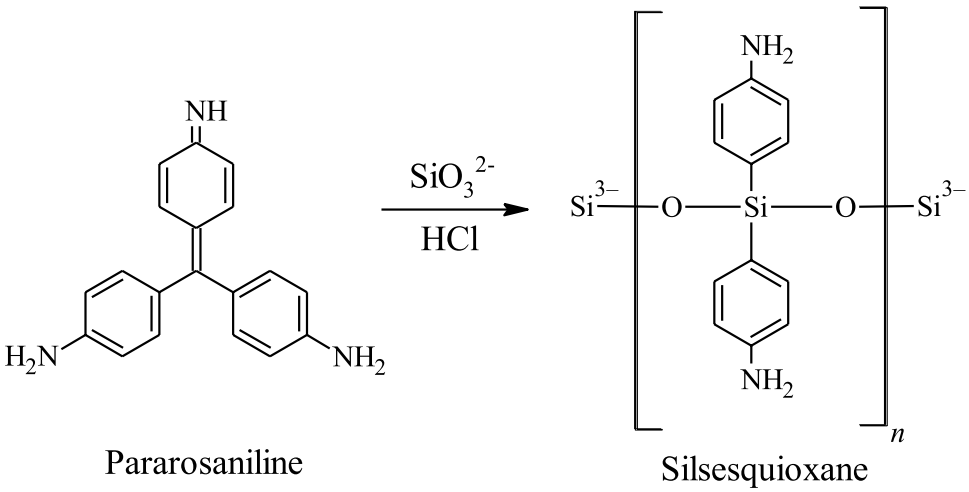

(6)

This performance is probably due to the bridging mechanism of SiO_3^{2-} as this substance reacts with destabilized PRA molecular intermediates and aggregates into large floc sizes to form an organosilicon tetrahedral polymer, silsesquioxane [24]. Subsequently, the pretreated (CF) PRA wastewater had undergone thermolysis treatment under various pH range and thermolysis temperature as revealed in Fig. 3b. As the pH increases from acidic (pH 2) to alkaline (pH 9) condition, the pretreated PRA only shows an additional slight color removal at which thermolysis temperature of 60 °C with additional 11% reduction and 90 °C with additional 12% reduction rate. The ANOVA analysis in Table 1 reveals that the initial solution of pH is significant ($p < 0.05$), whereas the temperature of thermolysis is not statistically significant ($p > 0.05$). Additionally, a wavelength scan was performed, and it can be seen from Fig. 3c that this phenomenon attributes to the cleaved structures have agglomerated into floc during the CF process and the complex structured floc is hardly breakable through thermolysis. The slight color reduction rate may due to the presence of chromophores intermediates that can further be degraded by thermolysis. Lastly, thermolysis reaction time under temperature 90° is taken into consideration. Obviously, there are no changes in color reduction rate from 25 min onwards as shown in Fig. 3d, which implies the prolonged reaction time does not destruct the complex structured floc formed during CF. Therefore, the maximum PRA reduction rate under CF–thermolysis is 60% at optimum operating parameters.

The combined thermolysis–CF treatment process promised a better PRA reduction compared to the combined CF–thermolysis process. This is because when thermolysis as the primary treatment, PRA was thermally cleaved and led to instability of the molecule structure. During the subsequent CF process, these cleaved molecules will tend to react with silifloc to form flocs through the bridging mechanism. Whilst for combined CF–thermolysis reflects poor PRA

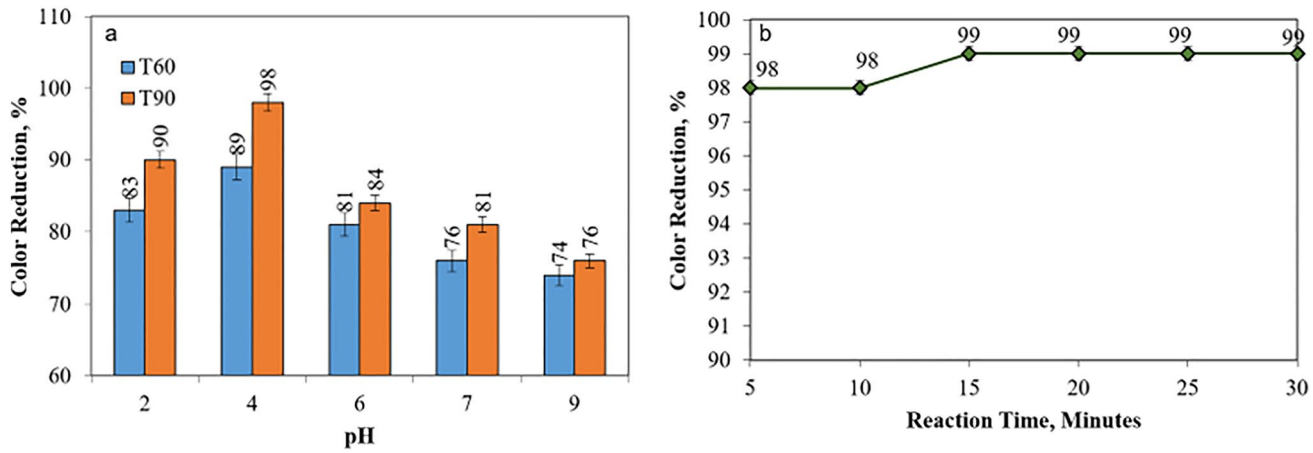

Fig. 4 Study of hybridized treatment. Effect of **a** PRA solution initial pH and **b** thermolysis reaction time on color reduction rates

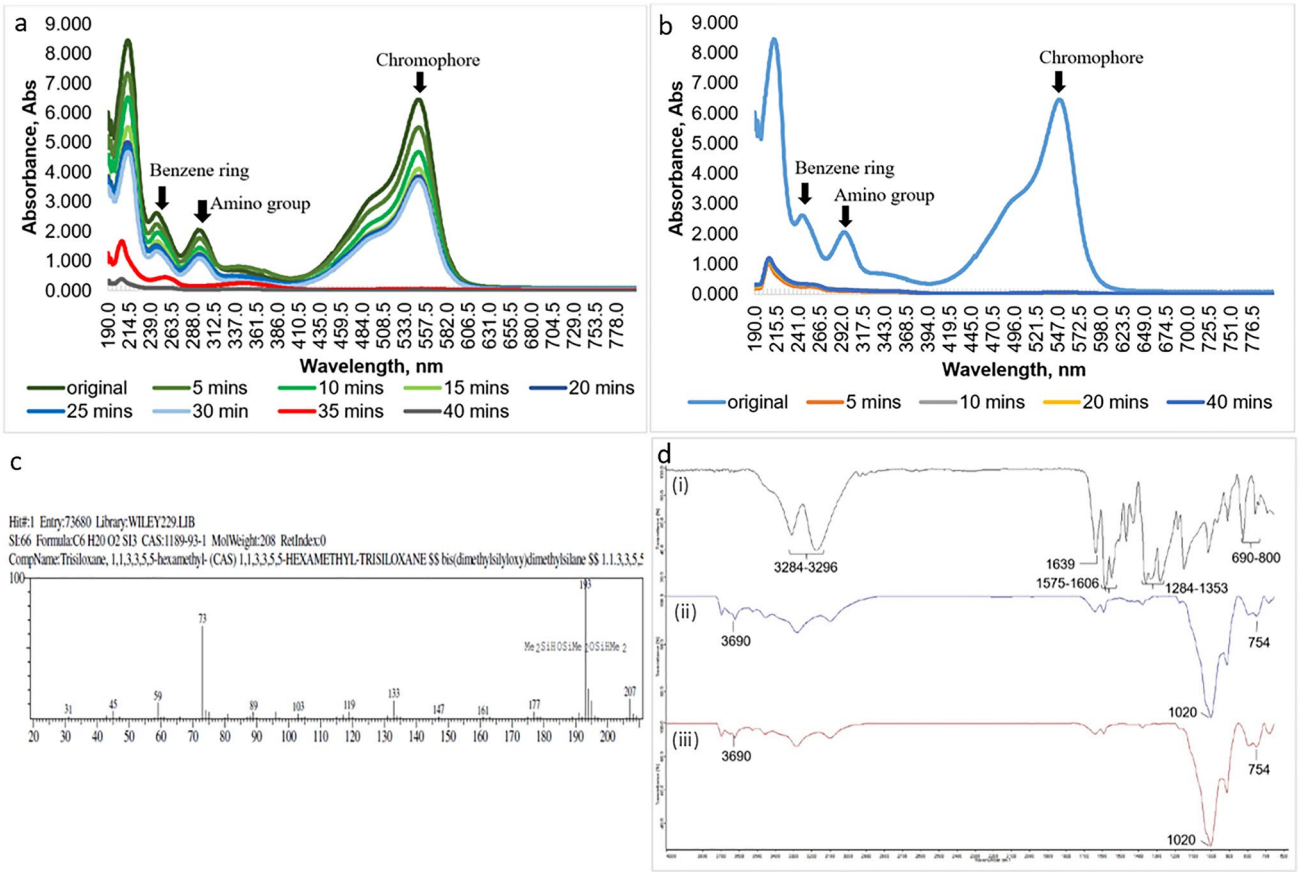

Fig. 5 **a** UV–Vis degradation kinetics of PRA for combined thermolysis–CF (conditions: initial pH solution of 9, thermolysis temperature of 90 °C, 50 mg/L of silifloc). **b** UV–Vis degradation kinetics of PRA for hybridized treatment (conditions: initial pH solution of 4, thermolysis temperature at 90 °C, 50 mg/L of silifloc). **c** GC–MS spectrum for silsesquioxane. **d** FTIR spectra of (i) PRA (ii) sludge after thermolysis–CF and (iii) hybridized treatment

reduction as during pre-treatment of CF, the destabilized molecules will adhere to form a larger and denser floc by forming complex ligands. The formation of the complex ligands is hardly breakable and more stable, therefore subsequent thermolysis process hardly observed any removal.

Hybridized treatment process performance study

When both thermolysis and CF processes were integrated and carried out simultaneously in a single vessel, the process is known as hybridized process [25]. Figure 4 summarizes the effect of pH and temperature in hybridized process, and the ANOVA analysis in Table 1c shows the significant relation of both operating parameters, initial pH and temperature. As displayed in Fig. 4a, when the pH varies from 2 to 4, PRA removal increases from 83 to 89% at 60 °C, whereas for 90 °C, removal increases from 90% at pH 2 to 98% at pH 4. As the basicity of the solution increases, removal shows a reduction of 15–22%, this phenomenon happens because with the presence of excessive hydroxide, silifloc tends to form $SiOH^{+}_{2}$, which inhibits the neutralization reaction with the cationic PRA. At the optimum pH of 4, both treatment methods were co-functioning simultaneously. The effect of reaction time is illustrated in Fig. 4b. During the initial 10 min, the color reduction rate is 98%. Further prolonged the reaction time to 30 min, the maximum color removal achieves is 99%. Therefore, the optimum conditions for the hybridized process were at initial pH solution of 4, thermolysis temperature at 90 °C and 10 min reaction time.

Mechanism and degradation study

From the PRA ability studies, it was found that hybridized process promises the best treatment efficiency compared to combined sequential processes. Further analysis was conducted for combined thermolysis–CF and hybridized processes to understand the degradation mechanisms of these two treatment processes.

Research on degradation roadmap for both treatment methods is evaluated through UV–Vis absorbance of PRA

by analyzing the molecular structure fragmentation at the respective wavelength bands. It can be seen in Fig. 5a, before reaction, PRA has a main band in the visible region located at 545 nm, which attributes to the chromophores that make up from ethenyl (–C=C–) and imino (–C=N–) groups [26]. Besides, the other absorption bands at 232 and 290 nm in the UV region are associated with the benzene ring and amino group, respectively [27].

During combined thermolysis–CF, as the reaction initiates by heating the PRA wastewater at 90 °C for 30 min, the visible band reduces gradually indicating fragmentation of chromophores with the presence of sufficient BDE. The first cleavage of PRA structure is ethyl group chromophores since bond enthalpy of ethyl group (356 kJ/mol) is lower compared to imino group (644 kJ/mol) [28, 29]. Breakage of ethyl group forms degradation intermediates of cyclohexa-2,5-dien-1-imine and 4,4'-methylenedianiline. Dissociation of energy further destabilizes 4,4'-methylenedianiline by producing sufficient enthalpy of reaction to attack the σ bond of –C–C– and decomposes to a more stable degradation substance, aniline [30]. Only a slight reduction in wavelength 232 and 290 nm indicates benzene structure in aniline compound that hardly thermal decomposed which accounted for insufficient heat is transferred to energy to scissor aniline with higher heat enthalpy of 770 kJ/mol [13, 31]. Subsequently, the pretreated (thermolysis) PRA wastewater

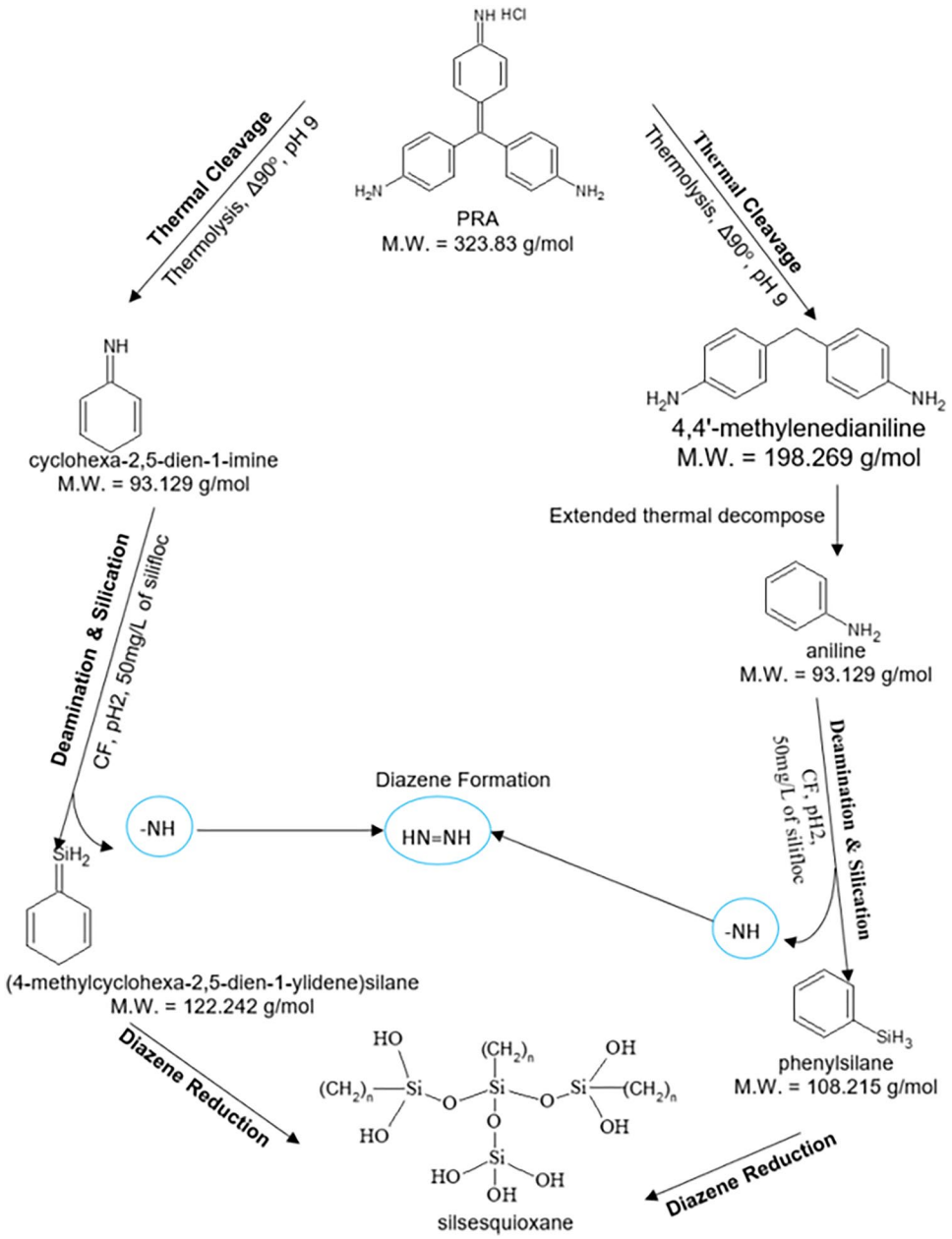

Fig. 6 PRA degradation mechanisms and attributes

proceeds with the CF process. Once the wastewater is coagulated by silifloc, an instant reaction is observed with a complete diminish of chromophores absorbance at 545 nm and sharp reduction of benzene ring and amino groups absorbance at 232 and 290 nm. It could be proposed that the degradation intermediates cyclohexa-2,5-dien-1-imine and aniline are easily cleaved at the –NH sides due to extended valence shell and their electron donating property. Silifloc facilitates the reaction of deamination to the formation of (4-methylcyclohexa-2,5-dien-1-ylidene)silane and phenylsilane through silication. Meanwhile, detachment of =NH tends to form diazene (HN=NH) which is a strong reducing agent for carbon–carbon double bond, (–C=C–) [32]. Diazene leads the fragment of –C=C– in benzene rings; hence, the aromatic ring decomposes to linear products of hydrocarbon, forming organo-bridged silsesquioxane.

On the other hand, during the hybridized treatment process, the UV–Vis degradation kinetics of PRA is depicted in Fig. 5b. A markedly spontaneous reaction took place within 5 min; the absorbance bands at visible region (545 nm) and ultra-violet region (290 and 232 nm) diminished entirely. This phenomenon indicates the complete decay of the PRA structure. Meanwhile, thermolysis thermally cleaves the PRA molecular structure, CF process reaction took place spontaneously on those cleaved molecules, which prevents the destabilized molecule intermediates to re-bind or form secondary products with other substances. The instant mineralization of PRA disallowed the degradation intermediates to be studied as the degradation happened rapidly. The identical UV–Vis degradation of combined thermolysis–CF and hybridized proposed a similar degradation mechanism with silsesquioxane as the degradation products. Diminishment of aromatic amine and formation of the final product, silsesquioxane is supported by GC–MS analysis as shown in Fig. 5c.

The evidence of the similarity degradation for thermolysis–CF and hybridization treatment is further supported by FTIR analysis with similarity up to 97.9%. FTIR spectra of PRA, sludge from thermolysis–CF and hybridized processes are illustrated in Fig. 5d. In the FTIR spectrum of PRA, the main intensity peaks corresponds to the following: 3284–3296 cm^{-1} represents the –NH stretching, 1639 cm^{-1} represents –C=C–, 1579–1606 cm^{-1} represents aromatic rings, 1284–1353 cm^{-1} represents –C–N– and 690–800 represents phenyl group of PRA, which are entirely diminished after treatment [33]. The disappearance in the functional groups was evident, confirming the reduction of PRA using thermolysis–CF and hybridized treatment. After both treatments, strong bands observed at the peaks 1000 cm^{-1} are related to the Si–O–Si asymmetry stretching vibration and 3690 cm^{-1} represents organosilicon structure [34] whereas a weak peak recorded at 754 cm^{-1} represents phenylsilane. This explained that the degradation final product, silsesquioxane, and the intermediates of phenylsilane previously undergo diazene reduction to form silsesquioxane. The overall degradation pathway is manifested in Fig. 6.

Conclusion

Combined sequential and hybridized processes of thermolysis and CF were employed to study the efficiency in treating PRA wastewater. Different operating conditions, such as temperature, pH, reaction time, silifloc dosage, were evaluated to optimize the treatment conditions for each of the treatment methods. Two conditions of combined processes in two sequential steps, thermolysis followed by CF and CF followed by thermolysis, were assessed. These two combined processes carried out at optimum operating parameters shows 86 and 60% of PRA reduction for thermolysis–CF and CF–thermolysis, respectively. The hybridized thermolysis–CF process gave the best result with 99% reduction. Further degradation kinetics of combined thermolysis–CF and hybridized process was evaluated. From the UV–Vis analysis, all the absorbance bands at visible region (545 nm) and ultraviolet region (290 and 232 nm) were completely diminished, which indicated complete mineralization of chromophores and auxochromes of PRA. The analysis result of FTIR supported the disappearance of PRA functional groups. The end degradation product with the formation of organo-bridged silsesquioxane was detected in GC–MS and FTIR.

Acknowledgements This work was supported by the Faculty of Civil Engineering Technology, Universiti Malaysia Perlis (UniMAP).

Author contributions All authors contributed to the study conception and design. Material preparation, data collection and analysis were performed by Y-YL, Y-SW, S-AO and NAL. The first draft of the manuscript was written by Y-YL and all authors commented on previous versions of the manuscript. All authors read and approved the final manuscript. Conceptualization: Y-YL; methodology: Y-YL; formal analysis and investigation: Y-YL; writing–original draft preparation: Y-YL; writing–review and editing: Y-SW; resources: Y-SW, S-AO, S-TS, K-ME, and T-TT; supervision: Y-SW, S-AO, and NAL.

Funding This fund is supported by Malaysia Ministry of Higher Education (Grant number FRGS/1/2015/TK02/UNIMAP/02/6).

Data availability All data generated or analyzed during this study are included in this publication.

Declarations

Conflict of interest The authors have no competing interests to declare that are relevant to the content of this article.

Ethical approval Not applicable.

Consent to participate Not applicable.

Consent for publication Not applicable.

References

1. Geissen V, Mol JGJ, Klumpp E, Umlauf G, Nadal M, van der Ploeg MJ, van der Zee SEATM, Ritsema CJ (2015) Emerging pollutants in the environment: a challenge for water resource management. Int Soil Water Conserv Res. https://doi.org/10.1016/j.iswcr.2015.03.002
2. Sathishkumar P, Palvannan T, Murugesan K, Kamala-Kannan S (2013) Detoxification of malachite green by *Pleurotus florida* laccase produced under solid-state fermentation using agricultural residues. Environ Technol. https://doi.org/10.1080/09593330.2012.689359
3. Adnan LA, Sathishkuma P, Yusoff ARM, Hadibarata T, Ameen F (2017) Rapid bioremediation of alizarin red S and quinizarin green SS dyes using *Trichoderma lixii* F21 mediated by biosorption and enzymatic processes. Bioprocess Biosyst Eng. https://doi.org/10.1007/s00449-016-1677-7
4. Li Y, Zhang Q, Li M, Sang W, Wang Y, Wu L, Yang Y (2020) Bioaugmentation of sequencing batch reactor for aniline treatment during start-up period: Investigation of microbial community structure of activated sludge. Chemosphere. https://doi.org/10.1016/j.chemosphere.2019.125426
5. Adnan LA, Hadibarata T, Sathishkuma P, Yusoff ARM (2015) Biodegradation pathway of Acid red 27 by white-rot fungus *Armillaria* sp. F022 and phytotoxicity evaluation. Clean: Soil, Air, Water. https://doi.org/10.1002/clen.201400249
6. Neumann H-G (2010) Aromatic amines: mechanisms of carcinogenesis and implications for risk assessment. Front Biosci. https://doi.org/10.2741/3665
7. Brüschweiler BJ, Kung S, Bürgi D, Lorenz M, Nyfelerc E (2014) Identification of non-regulated aromatic amines of toxicological concern which can be cleaved from azo dyes used in clothing textiles. Regul Toxicol Pharm. https://doi.org/10.1016/j.yrtph.2014.04.011
8. Mohammed M, Mekala LP, Chintalapati S, Chintalapati VR (2020) New insights into aniline toxicity: aniline exposure triggers envelope stress and extracellular polymeric substance formation in *Rubrivivax benzoatilyticus* JA2. J Hazard Mater. https://doi.org/10.1016/j.jhazmat.2019.121571
9. Koyuncu H, Kul AR (2019) Removal of aniline from aqueous solution by activated kaolinite: kinetic, equilibrium and thermodynamic studies. Colloids Surf A. https://doi.org/10.1016/j.colsurfa.2019.02.057
10. Karthikeyan S, Viswanathan K, Boopathy R, Maharaja P, Sekaran G (2015) Three dimensional electro catalytic oxidation of aniline by boron doped mesoporous activated carbon. J Ind Eng Chem. https://doi.org/10.1016/j.jiec.2014.04.036
11. Durán A, Monteagudo J, San Martín I, Merino S (2018) Photocatalytic degradation of aniline using an autonomous rotating drum reactor with both solar and UV-C artificial radiation. J Environ Manage. https://doi.org/10.1016/j.jenvman.2018.01.012
12. Sang W, Cui J, Feng Y, Mei L, Zhang Q, Li D, Zhang W (2019) Degradation of aniline in aqueous solution by dielectric barrier discharge plasma: mechanism and degradation pathways. Chemosphere. https://doi.org/10.1016/j.chemosphere.2019.02.029
13. Huang J, Ling J, Kuang C, Chen J, Xu Y, Li Y (2018) Microbial biodegradation of aniline at low concentrations by *Pigmentiphaga daeguensis* isolated from textile dyeing sludge. Int Biodeterior Biodegrad. https://doi.org/10.1016/j.ibiod.2018.01.013
14. Aleix B, Aida P, Lliberia JL, Gonzalez-Olmos R (2017) Degradation pathways of aniline in aqueous solutions during electrooxidation with BDD electrodes and UV/H_2O_2 treatment. Chemosphere. https://doi.org/10.1016/j.chemosphere.2016.09.105
15. Song S, He Z, Chen J (2007) US/O_3 combination degradation of aniline in aqueous solution. Ultrason Sonochem. https://doi.org/10.1016/j.ultsonch.2005.11.010
16. Ou B, Wang J, Wu Y, Zhao S, Wang Z (2019) A highly efficient cathode based on modified graphite felt for aniline degradation by electro-Fenton. Chemosphere. https://doi.org/10.1016/j.chemosphere.2019.06.144
17. Suresh R, Giribabu K, Manigandan R, Mangalaraja R, Solorza JY, Stephen A, Narayanan V (2017) Synthesis of Co^{2+}-doped Fe2O3 photocatalyst for degradation of pararosaniline dye. Solid State Sci. https://doi.org/10.1016/j.solidstatesciences.2017.04.005
18. Lau Y-Y, Wong Y-S, Ang T-Z, Ong S-A, Nabilah L, Ho L-N (2018) Degradation reaction of Diazo reactive black 5 dye with copper (II) sulfate catalyst in thermolysis treatment. Environ Sci Pollut Res Int. https://doi.org/10.1007/s11356-017-1069-9
19. Lau Y-Y, Wong Y-S, Teng T-T, Morad N, Rafatullah M, Ong S-A (2014) Coagulation-flocculation of azo dye acid orange 7 with green refined laterite soil. Chem Eng J. https://doi.org/10.1016/j.cej.2014.02.100
20. Su CX-H, Teng T-T, Wong Y-S, Morad N, Rafatullah M (2016) Catalytic thermolysis in treating cibacron blue in aqueous solution: kinetics and degradation pathway. Chemosphere. https://doi.org/10.1016/j.chemosphere.2015.12.048
21. Wang L, Wang X, Cheng J, Ning P, Lin Y (2018) Coupling catalytic hydrolysis and oxidation on Mn/TiO_2-Al_2O_3 for HCN removal. Appl Surf Sci. https://doi.org/10.1016/j.apsusc.2018.01.015
22. Chen L, Zhou CH, Zhang H, Tong DS, Yu WH, Yang HM, Chu MQ (2017) Capture and recycling of ammonium by dolomite-aided struvite precipitation and thermolysis. Chemosphere. https://doi.org/10.1016/j.chemosphere.2017.08.065
23. Sahu O (2017) Catalytic thermal pre-treatments of sugar industry wastewater with metal oxides: thermal treatment. Exp Therm Fluid Sci. https://doi.org/10.1016/j.expthermflusci.2017.03.022
24. Oladoja NA (2016) Advances in the quest for substitute for synthetic organic polyelectrolytes as coagulant aid in water and wastewater treatment operations. Sustain Chem Pharm. https://doi.org/10.1016/j.scp.2016.04.001
25. Grace Pavithra K, Senthil Kumar P, Jaikumar V, Sundar Rajan P (2019) Removal of colorants from wastewater: a review on sources and treatment strategies. J Ind Eng Chem. https://doi.org/10.1016/j.jiec.2019.02.011
26. Verma AK, Dash RR, Bhunia P (2012) A review on chemical coagulation/flocculation technologies for removal of colour from textile wastewaters. J Environ Manage. https://doi.org/10.1016/j.jenvman.2011.09.012
27. Ortiz E, Gómez-Chávez V, Cortés-Romero CM, Solís H, Ruiz-Ramos R, Loera-Serna S (2016) Degradation of indigo carmine using advanced oxidation processes: synergy effects and toxicological study. J Environ Prot. https://doi.org/10.4236/jep.2016.712137
28. Klein E, Lukeš V (2006) DFT/B3LYP study of O-H bond dissociation enthalpies of para and meta substituted phenols: correlation with the phenolic C–O bond length. J Mol Struct. https://doi.org/10.1016/j.theochem.2006.04.017
29. Berg JM, Tymoczko JL, Stryer L (2002) Biochemistry. WH Freeman, New York
30. Ouellette RJ, Rawn JD (2015) Organic chemistry study guide: key concepts, problems, and solutions. Elsevier, Netherlands
31. Laarhoven LJJ, Mulder P, Wayner DDM (1999) Determination of bond dissociation enthalpies in solution and in the gas phase. Acc Chem Res. https://doi.org/10.1021/ar9703443
32. Pasto DJ, Taylor RT (2004) Reduction with diimide, in organic reactions. John Wiley & Sons, New York

33. Duman O, Tunc S, Polat TG (2015) Determination of adsorptive properties of expanded vermiculite for the removal of C. I. basic red 9 from aqueous solution: kinetic, isotherm and thermodynamic studies. Appl Clay Sci. https://doi.org/10.1016/j.clay.2015.03.003
34. Karakuş S, Taşaltın N, Taşaltın C, Kilislioğlu A (2020) Comparative study on ultrasonic assisted adsorption of basic blue 3, basic yellow 28 and acid red 336 dyes onto hydromagnesite stromatolite: kinetic, isotherm and error analysis. Surf Interfaces. https://doi.org/10.1016/j.surfin.2020.100528

Authors and Affiliations

Yen-Yie Lau[1] · Yee-Shian Wong[1,2] · Soon-An Ong[1,2] · Nabilah Aminah Lutpi[1,2] · Sung-Ting Sam[3] · Tjoon-Tow Teng[4] · Kim-Mun Eng[5]

✉ Yee-Shian Wong
yswong@unimap.edu.my

[1] Faculty of Civil Engineering Technology, Universiti Malaysia Perlis, 02600 Arau, Perlis, Malaysia

[2] Water Research and Environmental Sustainability Growth, Centre of Excellence (WAREG), Universiti Malaysia Perlis (UniMAP), Arau, Perlis, Malaysia

[3] Faculty of Chemical Engineering Technology, Universiti Malaysia Perlis, 02600 Arau, Perlis, Malaysia

[4] Han Chiang University College, 11600 George Town, Penang, Malaysia

[5] Kenep Resources (Asia) Sdn. Bhd., No. 31 & 33, Persiaran Jelapang Maju 2, Taman Perindustrian Ringan Jelapang Maju, 30020 Ipoh, Perak, Malaysia